ELSEVIER

Journal of Alloys and Compounds 454 (2008) 483–490

Journal of ALLOYS AND COMPOUNDS

www.elsevier.com/locate/jallcom

Measurement of the reversible hydrogen storage capacity of milligram Ti–6Al–4V alloy samples with temperature programmed desorption and volumetric techniques

Jeff L. Blackburn [a,*], Philip A. Parilla [a], Thomas Gennett [b], Katherine E. Hurst [c], Anne C. Dillon [a], Michael J. Heben [a]

[a] *National Renewable Energy Laboratory, 1617 Cole Blvd, Golden, CO 80401, USA*
[b] *Chemistry Department, Rochester Institute of Technology, Rochester, NY 14623, USA*
[c] *National Institute of Standards, Boulder, CO 80305, USA*

Received 25 October 2006; received in revised form 3 January 2007; accepted 5 January 2007
Available online 11 January 2007

Abstract

We report the results of a study using temperature programmed desorption (TPD) and a volumetric sorption technique to measure the hydrogen storage capacity of the Ti–6Al–4V alloy. Samples of various sizes and surface treatments were studied to obtain a statistically meaningful value for the maximum hydrogen storage capacity, as well as to understand the effect of sample size, sample oxidation, and hydrogen charging conditions on the measured capacity. We find a maximum reversible hydrogen storage capacity of ∼3.76 wt% with hydrogen exposures near ambient temperature and pressure. This value is higher than any reported in the literature previously, possibly due to the utilization of very small particles and rapid hydrogen exposures, which allow for equilibration times of approximately 1 h. Comparison of a variety of samples indicates that the measured hydrogen capacity is affected by surface oxidation. Samples generated in a strongly oxidizing environment exhibit decreased hydrogen uptake. The implications of these results are discussed with regards to previously reported capacity values in the literature.

Keywords: Hydrogen absorbing materials; Metal hydrides; Titanium; Ti–6Al–4V; Temperature programmed desorption

1. Introduction

Titanium and vanadium alloys are promising candidates for the structural materials for nuclear reactors [1,2] and hydrogen storage media [3–5]. For both of these applications, an accurate measurement of the maximum hydrogen sorption capacity is extremely desirable. For nuclear reactors, this value plays a key role in the correct inventory of hydrogen isotopes. For hydrogen storage applications, an accurate measurement of the maximum capacity and absorption and desorption conditions are necessary for comparison to other metal hydride systems. One such material that has been studied by several groups is Ti–6Al–4V. The hydrogen uptake quoted in these studies, however, varies quite widely from ∼1.2 wt% to ∼3.4 wt% [1,5–7]. Addressing these discrepancies and determining the maximum hydrogen storage capacity of this material requires a detailed understanding of the various material and experimental parameters that may affect the hydrogen uptake kinetics and capacity.

The formation of a metal hydride begins with the mass transport of hydrogen molecules onto the solid–gas interface, dissociation of the molecules on the surface (chemisorption) at dissociation sites, and eventually, penetration of hydrogen atoms through the surface into the bulk [8]. The initial steps are highly dependent on the quality of the surface. For example, most hydride-forming metals and alloys are typically covered with a surface passivation layer (SPL). This SPL is not always well-defined, but consists of a combination of the metal oxides and hydroxides, formed through reaction with air and water, as well as carbon–oxygen compounds [8]. The SPL acts as a diffusion barrier to reduce the uptake rate of hydrogen, and also lowers the density of dissociation centers for hydrogen molecules.

Heat treatment in vacuum is typically used to overcome the kinetic limitations imposed by the SPL. Fresh metal surfaces become available during this heat treatment, as water and other

* Corresponding author.
E-mail address: jeffrey_blackburn@nrel.gov (J.L. Blackburn).

0925-8388/$ – see front matter © 2007 Elsevier B.V. All rights reserved.
doi:10.1016/j.jallcom.2007.01.006

volatile adsorbents are degassed, oxides are dissolved into the bulk of the metal, and the strain induced by lattice expansion causes fracture of the SPL [8]. Some of the oxidation, which results in the SPL, may be irreversible, rendering a portion of the sample inert to hydrogen uptake. Also, although dissolution of the SPL may enhance the rate of hydrogen uptake, oxygen dissolved into the bulk by heat treatment may occupy interstitial sites in the metal lattice, lowering the number of sites available to hydrogen, and may also lower the enthalpy of hydride formation [9–11].

Gaseous impurities may also lower the rate of hydrogen uptake or the hydrogen capacity for clean metals through reaction with the metal or alloy surface and concomitant generation of a SPL or removal of dissociation sites. This so-called "poisoning" effect may be especially significant at elevated temperatures, and has been demonstrated for gaseous impurities in both the adsorption and desorption processes. For example, traces of water, oxygen, and nitrogen have been shown to deactivate hydrogen uptake on titanium during absorption/desorption cycling [11,12]. Oxygen-containing impurities may be especially deleterious to titanium alloys, as they may promote the formation of titanium dioxide at elevated temperatures, rendering a portion of the alloy inert to hydride formation [11].

The formation of a surface hydride is followed by nucleation and growth of a true hydride phase once the hydrogen concentration in the metal or alloy exceeds the saturation concentration [8]. In most brittle intermetallic alloys, such as Ti–V–Al, the hydride density is lower than that of the parent alloy, and hydride formation is accompanied by stress fields and cracking of the parent alloy [13]. Thus, successive hydrogen absorption and desorption cycles will often cause bulk alloy samples to disintegrate into small particles, exposing fresh metallic surfaces and enhancing the kinetics of adsorption. However, this effect is troublesome for applications in which the alloy material should retain its structural integrity, and thus hydrogen embrittlement of titanium and vanadium alloys used for nuclear applications has been studied extensively in the literature [1,14].

Following nucleation and growth, the hydride phase propagates into the bulk of the metal or alloy. Experimentally, the time required to realize complete hydride formation for the sample will depend on the diffusion coefficient of hydrogen in the material, the activation energy associated with the phase transformation, the sample size, temperature, and pressure. The maximum hydrogen *capacity* of the material will depend on the amount of hydrogen sites that are still available for hydrogen occupation and the amount of sites that have been removed or disabled by other processes, such as dissolution of the SPL, the formation of a stable oxide, or poisoning.

The majority of studies undertaken with the Ti–6Al–4V alloy have been performed on bulk samples with correspondingly large diffusion lengths. Thus, any experiments at low temperature tend to suffer from prohibitively long equilibration times, [14] whereas high temperatures and pressures may be used to hydrogenate the alloy in a more reasonable amount of time. Charging at high temperature and pressure is undesirable for hydrogen storage applications, as these energetic inputs lower the net energy density associated with any metal hydride system. One possible solution to the diffusion limitation is to use small particles where small diffusion lengths allow for quick equilibration times. However, small particles have high surface areas, leading to other practical issues such as surface passivation, poisoning, and adsorption barriers. Hence, if small particles are used to bypass the kinetic limitations for hydrogen absorption/desorption, it is necessary to understand surface effects on the hydrogen uptake kinetics and storage capacity.

In this study, we use temperature programmed desorption (TPD) and a volumetric "Sieverts" apparatus to measure the maximum hydrogen storage capacity of Ti–6Al–4V alloy particles near ambient temperature and pressure. We also examine pure titanium and titanium hydride samples as standards to ensure that calibration is maintained throughout the experiments, and that the capacity value measured is accurate to within a relative error of 2%. Rapid hydrogen exposure, using small alloy particles, that is $\leq$45 μm, allows for the absorption of hydrogen at standard temperature and pressure, with equilibration times on order of 1 h. We find a maximum reversible hydrogen storage capacity of ∼3.76 wt% for Ti–6Al–4V loaded with hydrogen at 300 K and 500 Torr, a value higher than any reported in the literature previously. We also examine a variety of samples generated in a strongly oxidizing environment to determine the effects of surface oxidation. These measurements are consistent with an expected inverse correlation between the amount of sample oxidation and the hydrogen storage capacity.

2. Experimental

Pure Ti–6Al–4V alloy powder was obtained from Goodfellow (www.goodfellow.com, Ti90/Al6/V4, catalog #TI016021 and #TI016010) and consisted of particles no larger than 45 μm and 450 μm, respectively. Ultrasonic horn tips from Cole Palmer are also made from the Ti–6Al–4V alloy. When used to sonicate acidic solutions, these horn tips degrade over time, ejecting alloy particles with high surface area and a large size distribution, ranging from tens of nanometers to hundreds of microns [6]. To examine the effect of oxidation on the hydrogen storage capacity of the alloy, we generated tip alloy particles in a strongly oxidizing environment of 3 M nitric acid. The horn tip was placed ∼2 in. into a graduated cylinder containing 20 ml of 3 M nitric acid solution. The power on the Cole Palmer control module was set to 650 W, and the horn was allowed to operate for 12–48 h, generating a slurry of alloy particles in the acidic solution. This slurry was centrifuged at 3900 rpm for ∼30 min, after which the acidic supernatant was decanted off of the precipitate of alloy particles. Excess acid was removed by adding 20 ml of de-ionized water to the alloy particles and repeating the centrifuge step. This washing was repeated three times, after which the alloy particles were dried and collected. Typical yields were on the order of 5 mg for 12 h of sonication. A Mettler-Toledo UMT2 microbalance with a readability of 0.1 μg and a repeatability of 0.25 μg was used to determine the weight of each sample which was weighed three times. The sample masses for titanium and Ti–V–Al powders were in the range of 0.5–2 mg. Consequently, the weight of each ∼1 mg sample is well known to at least 1%.

The TPD and volumetric apparatuses have been described in detail previously [6]. For TPD measurements, samples were loaded into a platinum packet, which was placed in a quartz tube and secured onto an external port of the TPD apparatus. The sample tube was cooled via a liquid nitrogen dewar and heated with a small resistively heated furnace. Prior to TPD, all samples were initially degassed in a vacuum of $\sim 10^{-8}$ Torr by ramping the temperature from room temperature to temperatures between 823 and 973 K at a rate of 1 K/s. The mass spectrum of desorbed species was monitored in the range of 1–50 amu. Samples were then treated with room temperature hydrogen exposures at a pressure of 500 Torr. We note that the hydrogen dose is introduced into the sample chamber quickly, over the course of ∼20 s. The fast introduction of hydrogen is very

important, as slow introduction, that is a slow leak into the chamber, does not allow for the full extent of hydrogenation in a reasonable time. This will be discussed in detail shortly. Following the initial charging, the sample was left under hydrogen atmosphere for approximately 1 h. The sample was then cooled to 95 K with the hydrogen overpressure. Hydrogen was then evacuated at 95 K to achieve a final base pressure of $1–4 \times 10^{-8}$ Torr. The samples were then heated linearly to 823–973 K at a nominal heating rate of ∼1 K/s, and the effluence of hydrogen was measured with the mass spectrometer as a function of sample temperature. This signal, being previously calibrated, was converted to moles-H_2/s and integrated to provide the amount of hydrogen stored.

The TPD apparatus was calibrated by a primary standards technique recently developed in our group [15]. This is a flow calibration technique relying on highly pure hydrogen gas, and not desorption of hydrogen from secondary standards such as titanium hydride. Our capacity measurements on pure titanium (Alfa Aesar #10386) and titanium hydride (Alfa Aesar #89183) samples were used to verify the accuracy of this calibration. Several TiH_2 samples were also measured throughout the course of experiments on alloy samples to serve as "spot checks" to ensure consistent calibration was maintained. We utilize the Sandia National Laboratories Hydride Properties Database to provide the accepted theoretical capacity of metal hydride systems [16]. The hydrogen capacity of a metal hydride material is defined as follows:

$$\text{wt\%} = \frac{\text{wt (H)}}{\text{wt (M + H)}} \times 100 \quad (1)$$

where H represents hydrogen atoms and M represents all metal atoms in the compound. For example, in the case of alloys, the weight of all metal atoms must be counted, even if they do not form a bulk metal hydride. For titanium hydride, the database gives a stoichiometry of $TiH_{1.97}$, yielding a capacity of 3.98 wt%.

The measurement procedure used for the volumetric apparatus was similar to that of the TPD where upon loading and evacuating the sample container, the sample was degassed by heating under vacuum to ∼773 K. Once the sample had cooled to room temperature, hydrogen was introduced at ∼500 Torr and allowed to absorb into the sample for a period of time. With the volumetric apparatus, this absorption could be monitored by recording the pressure as a function of time. Subsequent quenching with liquid nitrogen "immobilized" the absorbed hydrogen by drastically lowering the diffusion constant and the overpressure of hydrogen was then evacuated. The temperature of the sample was then quickly increased to 873 K and as the pressure increased, the hydrogen was counted by repeating the process of isolating aliquots in a known volume at measured temperature and pressure to determine the number of moles. After the moles were counted for each aliquot, the known volume was evacuated, and then replenished with hydrogen from the sample. As the sample pressure fell below ∼0.5 Torr, the temperature was increased to 923 K to facilitate the desorption of the hydrogen and hasten this mole counting procedure.

Thermal gravimetric measurements were performed on a TA Instruments simultaneous DTA/TGA (model SDT 2960). The temperature was ramped up at 20 °C/min to 1400 °C under a dry gas mixture of 80% N_2 and 20% O_2 (∼ "air") at a total flow of 100 sccm. The X-ray diffraction (XRD) diffractometer is a Scintag PTS 4-circle Goniometer with a Cu target operated at 45 kV and 36 mA (∼1.6 kW) and a solid-state liquid nitrogen-cooled Ge X-ray detector. The samples were in powder form and were attached to a low background quartz substrate by using a few drops of a mixture of Duco cement (10 wt%) and acetone (90 wt%). The glue is amorphous when dry, and adds almost no background signal. Data were collected from 5 to 125 degrees two theta (2θ) in 0.05 degree steps with the following scan rates: 1.2, 0.2 and 0.055 degrees per minute for 450 μm, 45 μm and horn materials, respectively.

3. Results

3.1. Titanium and titanium hydride samples

An appropriate standard must be utilized to ensure proper calibration of both the TPD and volumetric apparatuses. We utilized titanium hydride powder to ensure constant calibration within 2% for both techniques. For TPD measurements, capacities for each sample are calculated by integrating the area under the H_2 desorption curve, which was calibrated by the flow technique, the details of which can be found elsewhere [15]. A number of titanium hydride powders were decomposed to rigorously check the flow calibration technique. Following this decomposition, TiH_2 samples may be reversibly hydrogenated to the initial capacity; however the average value reported here corresponds solely to the decomposition measurements.

Measurements on eleven TiH_2 samples produced an average hydrogen capacity of 4.00 ± 0.032 wt%. The standard deviation (S.D.) for this average corresponds to a relative error of 0.80%, while the average value corresponds to a 0.50% error relative to the accepted value of 3.98 wt%. These numbers attest to the accuracy and precision of the flow calibration for determining

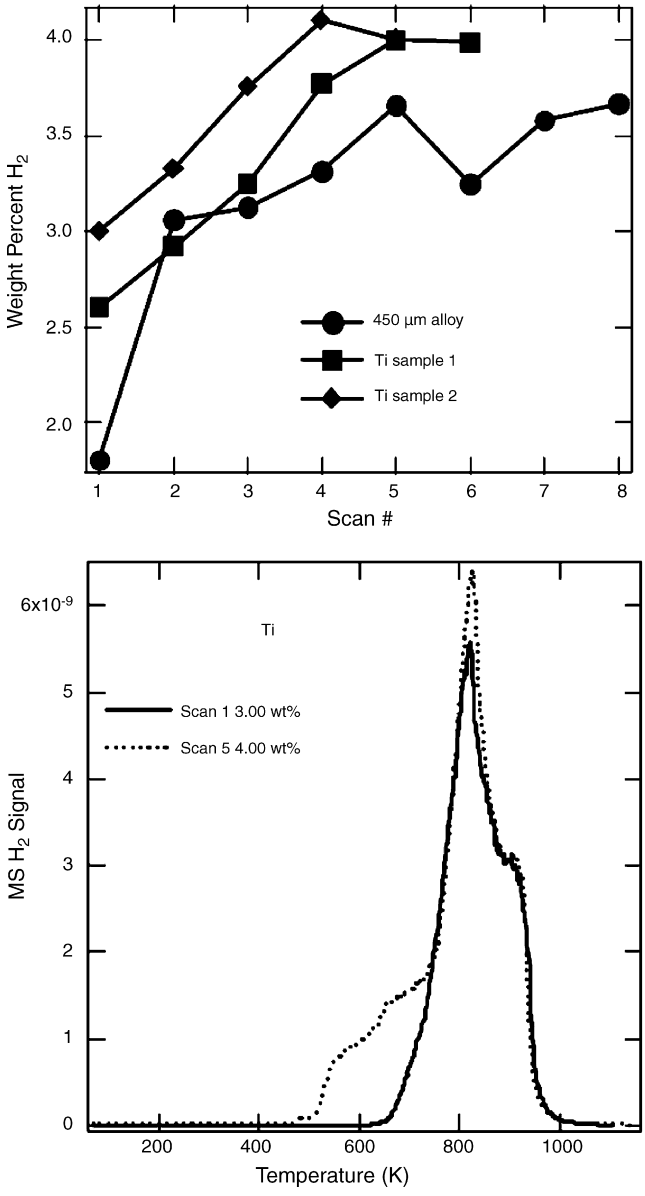

Fig. 1. (a) Hydrogen capacities measured from hydrogen desorption as a function of cycle number for titanium powders and 450 μm Goodfellow alloy powder. (b) First and fifth TPD spectra for titanium powder, taken at a heating rate of 1 K/s.

the hydrogen capacity of milligram samples. The decomposition of TiH_2 was also used to test the accuracy of the volumetric apparatus. The average value calculated for the volumetric apparatus for four samples was 3.99 ± 0.080 wt%. This S.D. corresponds to a relative error of 2.0%, with an error of 0.30% compared to the accepted value of 3.98 wt%. It is evident that the calibrations for both systems yield a stoichiometry very close to the accepted value of $TiH_{1.97}$.

The importance of the activation process is demonstrated with the titanium powder samples, which did not show the maximum hydrogen uptake on the first absorption/desorption cycle. Fig. 1a shows the capacity of two titanium powder samples. It is evident that the capacities begin very low, as low as 2.6 wt%, but climb to the theoretical value over the course of several cycles. The possible causes of this "activation" will be discussed in detail shortly. Interestingly, Fig. 1b shows that the increase in capacity coincides with an increased desorption of hydrogen at lower temperatures.

The close agreement of the capacities of the TiH_2 samples and the "activated" Ti samples to the theoretical capacity of 3.98 wt% demonstrates that under the conditions we use, we are able to reversibly hydride Ti to the maximum stoichiometry of $TiH_{1.97}$. We also note the absence of extreme kinetic limitations for charging either type of sample (once titanium has been activated). Charging the titanium samples for 1 h resulted in the maximum hydrogen capacity.

3.2. TPD and volumetric measurement of maximum alloy capacity

The 45 μm and 450 μm alloy particles from Goodfellow were measured on the TPD and volumetric apparatuses to determine the maximum capacity of the alloy. Fig. 1a shows that an "activation" phenomenon occurs for the 450 μm alloy, similar to what is seen for the titanium powders. These particles start with a very low capacity of ~1.8 wt% in the first cycle, and saturate at a capacity of ~3.6 wt% after five cycles.

The 45 μm alloy particles were measured on both the TPD and volumetric apparatuses. The absorption step may be monitored in real time with the volumetric apparatus. In the volumetric apparatus, after the degas and introduction of hydrogen for the first time, it was observed that little or no absorption occurred. Only upon raising the sample temperature to more than 673 K, did the sample absorb the hydrogen. Subsequent runs then showed absorption occurring at room temperature. Furthermore, the time to reach equilibrium was slower for the first run and became much faster with additional runs. A similar temperature window was observed previously for activation of the Ti–6Al–4V for hydrogen absorption [5]. The results for the desorption capacities of the 45 μm alloy are listed in Table 1, which lists nine measurements for three samples with each sample measured three times. Measurements for two of the samples occurred using the volumetric technique while the third used TPD. These particles show highly reversible hydrogen absorption under the experimental conditions, with the capacity remaining constant near a value of ~3.76 wt%. The measurements show good consistency with the exception of one outlier point, which is the first charging of the TPD sample. This low value was caused by not letting the sample reach full equilibrium with the hydrogen as the charging time was 1 h and, being the first charge, this Goodfellow sample had slower kinetics as observed in the volumetric experiment. For completeness and comparison, averages were calculated with and without this outlier to gauge its effect on the outcome. The table shows averages with the outlier included (in italics) and excluded (in bold). The uncertainty associated with the averages is the standard deviation with the relative error in the last column (both 1σ). From these data, the best value for the capacity of the Ti–Al–V alloy under these charging con-

Table 1
Lists the results of hydrogen storage capacities for the 45 μm Ti–Al–V Goodfellow alloy

Sample name	Technique	Run #	H_2 capacity (wt%)	Relative error (%)
Ti–Al–V V1	Volumetric	1	3.77	
Ti–Al–V V1	Volumetric	2	3.83	
Ti–Al–V V1	Volumetric	3	3.79	
Average for Ti–Al–V V1	Volumetric	Average	3.797 ± 0.031	0.82
Ti–Al–V V2	Volumetric	1	3.76	
Ti–Al–V V2	Volumetric	2	3.68	
Ti–Al–V V2	Volumetric	3	3.73	
Average for Ti–Al–V V2	Volumetric	Average	3.723 ± 0.040	1.07
Average for both volumetrics	Volumetric	Average	3.760 ± 0.051	1.36
Ti–Al–V *T1*	*TPD*	*1*	*3.56*	
Ti–Al–V T1	TPD	2	3.75	
Ti–Al–V T1	TPD	3	3.76	
Average for #2 and #3	**TPD**	**Average**	$\mathbf{3.755 \pm 0.007}$	**0.19**
Average for #1, #2 and #3	*TPD*	*Average*	3.690 ± 0.113	*3.06*
Average for volumetric and TPD-T#1			$\mathbf{3.759 \pm 0.044}$	**1.17**
Average for volumetric and TPD			3.737 ± 0.078	*2.09*

Highlighted in italics are an outlier point, Ti–Al–V T1, run #1, as well as averages that use the outlier point. Averages without the outlier are in bold. See text for further discussion. The average representing the best value for alloy capacity is in bold text at the bottom of the table.

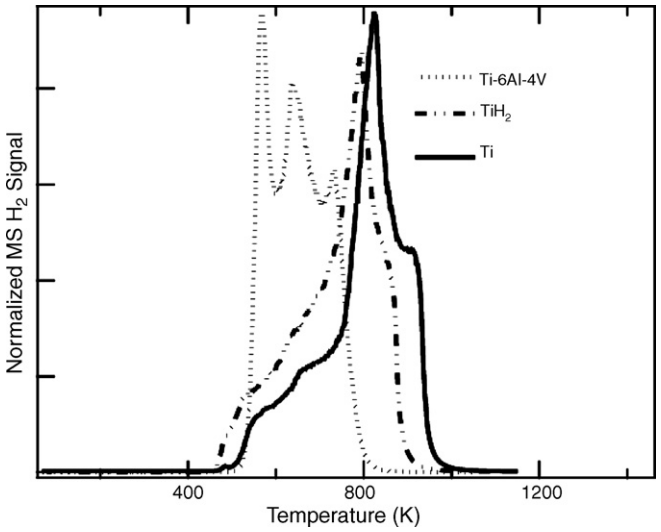

Fig. 2. Comparison of temperature range of H_2 desorption for Ti, TiH_2, and Ti–6Al–4V samples from TPD. The spectrum shown for each sample is taken after hydriding at 500 Torr, and after each sample has reached its maximum capacity. Thus, this is the second scan for the TiH_2 sample, the first being the decomposition of the pure TiH_2. The spectrum for the Goodfellow alloy is the first desorption spectrum, while that shown for Ti is the fifth desorption spectrum.

ditions is 3.759 ± 0.044 (1σ). Surprisingly, this value is much higher than previously reported in the literature [1,5–7], and also higher than the maximum hydrogen capacity found for the 450 μm alloy particles. Thus, the smaller 45 μm particles are the most appropriate sample to measure the *maximum* hydrogen capacity for the Ti–6Al–4V alloy, as discussed below.

Fig. 2 shows the TPD spectra for the Goodfellow 45 μm alloy, pure titanium hydride powder, and titanium powder. The major difference that alloying makes is to lower the temperature of hydrogen desorption. For the titanium and titanium hydride samples, the majority of desorption occurs between 673 and 873 K, while for the alloy, the bulk of desorption occurs between 473 and 673 K. For both the titanium and titanium hydride samples, some desorption occurs between 473 and 673 K. However, the majority of desorption still occurs at much lower temperatures for the alloy. Lower desorption temperature is a desirable feature for hydrogen storage applications, as it increases the net energy that may be extracted from a metal hydride system by lowering the operating temperature needed to desorb hydrogen.

3.3. Effect of oxidation on alloy capacity

In an effort to study the effects of sample oxidation on absorption capacity, we generated samples in a highly oxidizing environment. The oxidized samples were studied by thermogravimetric analysis (TGA) and X-ray diffraction (XRD), and compared to the "un-oxidized" 45 μm Goodfellow particles.

The as-received 45 μm alloy was used to calculate the maximum possible un-oxidized alloy content. TGA results in "air" (20:80 O_2:N_2), ambient up to 1400 °C, are listed in Table 2. The mass increase from combustion in air results from conversion of the components in the alloy to the corresponding metal oxides. *Stoichiometric* conversion of the entire alloy sample requires

Table 2
Lists the results of TGA in "air" of pure Ti–Al–V alloy

	Description	
	Mass increase (%)	Uncertainty
Theoretical	**167.97**	**±0.63**
Sample A	170.20	±0.20
Sample B	169.60	±0.30
Sample C	167.80	±0.20
Sample D	168.35	±0.15
Average of samples	**168.99**	**±1.10**

The uncertainty associated with the theoretical value reflects the uncertainty in the oxidation of vanadium. The uncertainty of the average is the standard deviation of the values.

that the entire sample be free of oxides before combustion. If a portion of the alloy is already oxidized before combustion, then the mass increase measured will only correspond to that of the unoxidized fraction, and a value lower than the theoretical value will be measured. The average of the TGA samples and the theoretical value (bold in table) agree within 0.6% relative difference and are well within the uncertainties indicating that the as-received samples are unoxidized. XRD of the TGA residues showed the primary phase present was TiO_2 followed by roughly equal quantities of Al_2O_3 and Al_2TiO_5. The Al_2TiO_5 phase showed peaks slightly shifted from their normal positions and may be indicative of some V substitution although this is not confirmed. Otherwise there is no indication of the vanadium oxidation state, which leads to a small uncertainty in the predicted mass increase. Note that the Al_2TiO_5 phase is equivalent stoichiometrically to $TiO_2 + Al_2O_3$, and its presence does not affect the predicted TGA mass increase from oxidation.

Alloy particles generated from the ultrasonic horn tip were then examined to gauge the effect of oxidation on the hydrogen storage capacity. The particles obtained by this method are ejected from the horn tip during sonication in 3 M nitric acid solution, and are expected to have oxide layers with thicknesses depending on the synthesis conditions. The use of a cooling bath around the graduated cylinder resulted in samples with higher hydrogen capacities than those obtained for cylinders that were not cooled. Three samples were generated with the cooling bath that showed an average reversible hydrogen storage capacity of $3.72 \pm 0.14\%$. This suggests that the alloy may retain close to the maximum capacity of ~3.76%, even in the strongly oxidizing environment of the nitric acid solution.

XRD measurements of the 45 μm Goodfellow alloy, the 450 μm Goodfellow alloy, and the ultrasonic horn alloy produced from sonication are shown in Fig. 3. All share common diffraction peaks from Ti–Al–V. The crystal structure is consistent with being hexagonal, isomorphic with titanium but with shifted lattice constants. For pure titanium, $a = 2.951$ and $c = 4.685$ Å, while for the alloy $a = 2.921$ Å and $c = 4.665$ Å. This XRD data and previous compositional analysis on the horn show that the horn material and Goodfellow alloys are essentially identical materials with respect to the metal composition. In addition, Fig. 3 shows that the extracted horn material contains an oxidized fraction (arrows) due to the oxidizing environment of the

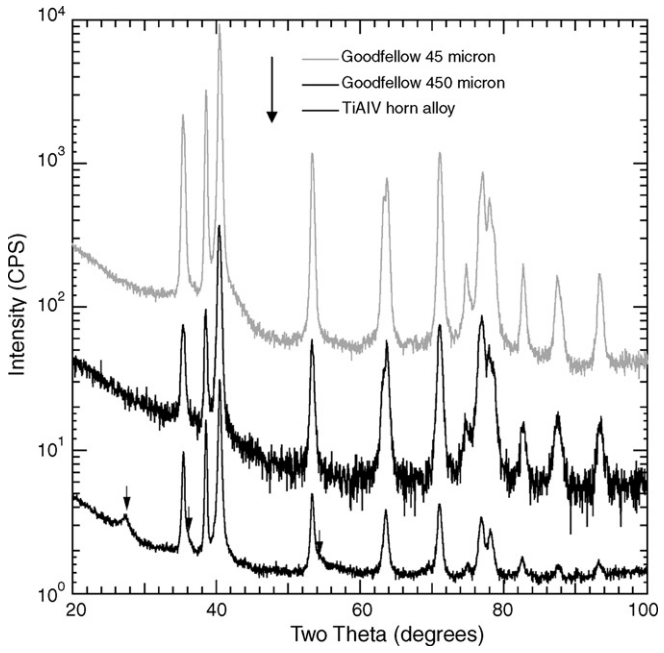

Fig. 3. Compares the XRD of three alloy samples: the 45 μm Goodfellow, the 450 μm Goodfellow, and an alloy sample produced from sonication in a nitric acid bath. All the three samples show the identical peaks from the Ti–Al–V alloy. The sonicated horn sample also shows a minor component of the TiO_2 rutile phase; the arrows mark the location of the three strongest intensity peaks for this rutile phase. The curves have been offset for clarity.

nitric acid bath during its production. This suggests that the permanent irreversible oxidation of the sample may occur, which lowers the hydrogen storage capacity.

The amount of oxidation can be correlated with TGA measurements in air and hydrogen desorption measurements (from TPD) as is shown in Fig. 4. The data show that the increase to the final oxidation weight in the TGA is directly correlated to the hydrogen capacity. This is expected since a low TGA mass increase signifies that the sample already has a significant oxidized fraction that cannot store hydrogen. Conversely, a large TGA mass increase means that most of the sample is unoxidized and can fully participate in storing hydrogen. Based on the H_2 capacity obtained from the pure Goodfellow alloy (3.759 ± 0.044 wt%), one can predict the relation between the TGA mass increase and the H_2 capacity, and this curve has been added to the figure. There are no free parameters for this curve and the experimental data agree well with the predicted curve. The dotted lines bounding the predicted curve and the theoretical maximum increase show the uncertainties associated with these calculations. These data show that the oxide layer does indeed diminish the hydrogen capacity on the horn-produced samples.

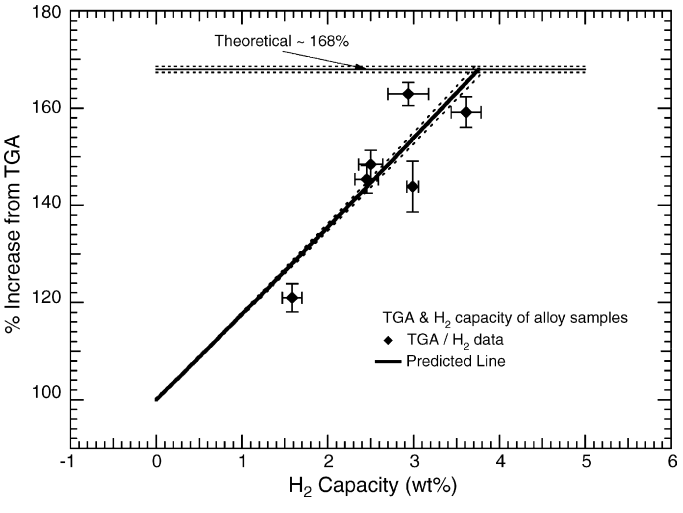

Fig. 4. Percent mass increase due to oxidation in "air" versus H_2-storage capacity data shows the expected correlation due to an oxide coating on the alloy particles. The line shows the predicted correlation with no free parameters and using the measured H_2 capacity from the pure Goodfellow alloy. The flat line at 167.97% shows the maximum theoretical TGA mass increase. The dotted lines near the predicted and theoretical lines represent the uncertainties in those calculations.

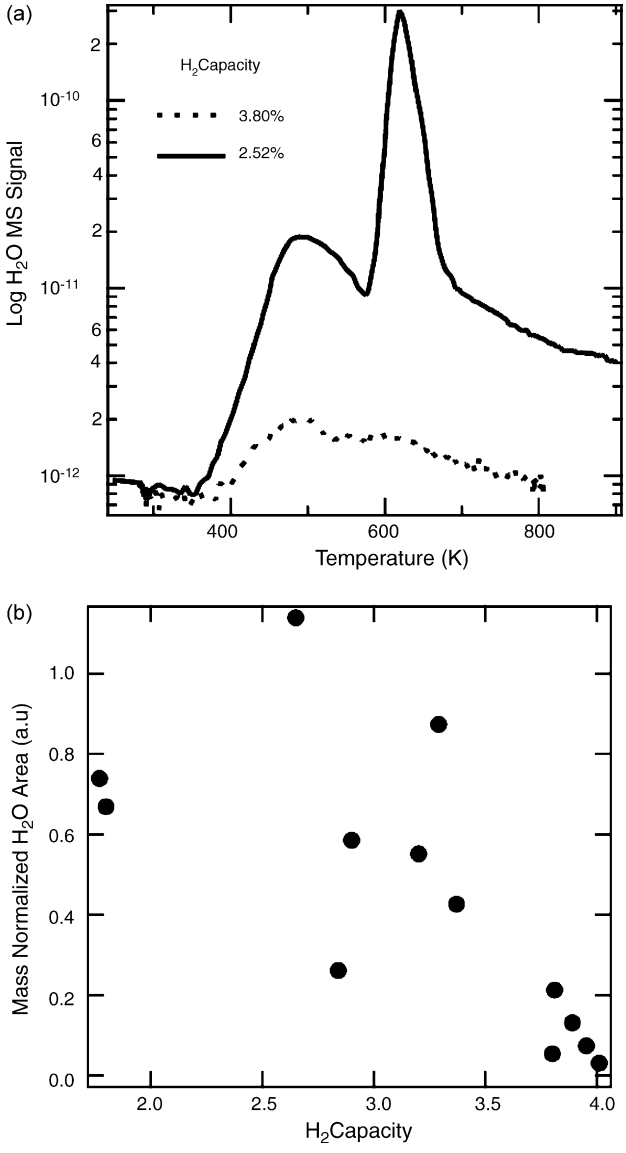

Fig. 5. (a) Comparison of H_2O degas spectrum for two different alloy samples generated from an ultrasonic horn tip. Note the MS signal on the *y*-axis is plotted on a log scale. (b) Mass normalized area for the water degas spectrum as a function of H_2 capacity for 13 different horn alloy samples shows that the water signal is inversely correlated with the hydrogen capacity.

Finally, we note that a strong correlation exists between the hydrogen storage capacity of the horn-generated alloy particles and the amount of water desorbed during the initial degas. Fig. 5a shows the H_2O degas spectrum of two horn alloy samples, one with a high capacity and another with a low capacity. The amount of water desorbed (mass-normalized) from the low capacity sample is approximately two orders of magnitude higher than for the high capacity sample. The area under the H_2O degas curve was integrated for many samples and normalized to the mass of the sample; the results are plotted in Fig. 5b. Despite the large amount of scatter in the plot, an inverse relationship is clearly observed between the amount of water desorbed in the degas step and the storage capacity.

4. Discussion

The initially low capacity of the Ti powder and 450 μm alloy particles, as well as the subsequent increases with cycling, can be attributed to an activation behavior that may have multiple causes. For one, as discussed above, the surface of these samples will normally be coated with an SPL, which would hinder hydride formation. Repetitive heat treatment under high vacuum removes this SPL, exposing fresh metal surfaces for hydrogen absorption [17]. Also, titanium and titanium-based alloys suffer from embrittlement from the lattice expansion associated with hydrogen absorption [1,14]. Thus, it is possible that the first few absorption/desorption cycles create micro-cracks in the titanium or Ti–6Al–4V particles thereby exposing fresh metallic surfaces [1]. This micro-structural rearrangement would increase the metal surface area available, enhancing the kinetics for hydrogen absorption [4].

Despite the increase with cycling, the capacity for the 450 μm particles still saturates at 3.6%, below the highly reproducible value of ∼3.76% for the 45 μm particles. It is possible that kinetics play a role with these larger particles. The particles may be large enough that diffusion path lengths pose a problem, even for the "activated" sample, for reaching equilibrium in the charging time (∼1 h) at room temperature and ∼1 atm. Considering diffusion into a spherical volume, the time necessary to reach saturated absorption is proportional to the square of the sphere's radius, and inversely proportional to the diffusion coefficient, $t \propto r^2/D$ [18]. Thus, it would take one hundred times longer for the ∼450 μm particles to saturate than the ∼45 μm particles. Assuming an approximate diffusion coefficient of $\sim 1 \times 10^{-9}$ cm^2/s, one can calculate that the ∼45 μm particles should be saturated with hydrogen in approximately 1 h, while the ∼450 μm particles would take nearly 100 h [18].

Given the fact that the 450 μm particles saturate near the value achieved for the 45 μm particles in only 1 h, it is clear that the saturation time is not 100 h. This is where the importance of the rapid introduction of hydrogen, as employed in these experiments, becomes apparent. A Ti–6Al–4V sample was placed in an internal Pt packet [6] where the packet temperature may be directly monitored via a thermocouple. Upon the rapid introduction of hydrogen into the sample cell, we observe a transient increase in the Pt packet temperature of a few degrees celsius. This temperature increase is due to the exothermic reaction of hydrogen with titanium

$$\mathrm{Ti} + \mathrm{H_2} \rightarrow \mathrm{TiH_2}, \qquad \Delta H = -125\,\mathrm{kJ/mol}$$

This rapid release of heat from the sample produces a transient enhancement in the diffusion coefficient of hydrogen, with the degree and duration of the enhancement determined by the heat capacity of the surroundings. We suspect that the transient temperature rise for the individual particles is much larger than a few degrees but is quickly dissipated. Because the time to reach saturated absorption is inversely correlated to the diffusion coefficient, this lowers the saturation time significantly. The overpressure of hydrogen (≤500 Torr) both amplifies the magnitude of this heat pulse, and also leads to the rapid uptake of significant quantities of hydrogen that would not be realized if the hydrogen was slowly leaked into the sample chamber. This rapid enhancement of the diffusion coefficient, along with the utilization of very small particle sizes, explains how we are able to charge the Ti–6Al–4V alloy to its maximum capacity at near ambient temperatures in approximately 1 h. Previous experiments have required higher temperatures and longer exposure times, and have not achieved the capacity realized in our experiments [1,5,14]. The effect of the temperature transient does not appear to influence the final hydrogen capacity except through its influence on the diffusion constant, that is, higher temperatures usually result in a lower hydrogen capacity and here we have measured the highest capacity yet for this alloy.

The largest disadvantage to using small particles is their correspondingly high surface area to volume ratio when compared to larger particles. A high surface area means that a larger fraction of the sample consists of a highly reactive surface with a large driving force for oxidation. For the as-received Goodfellow alloy particles, oxidation in ambient atmosphere does not significantly affect the hydrogen absorption. This is evidenced by the fact that the 45 μm particles, which should have a larger surface area to volume ratio than the 450 μm particles, yield a higher absorption capacity.

The effect of oxidation is clearly evident for samples generated in nitric acid, as shown in Fig. 4. We stress here that the capacities measured for the samples shown in Fig. 4 are the reversible capacities. These samples were cycled to see if any increase in the capacity, or "activation", occurred, similar to that observed for titanium powder and the Goodfellow 450 μm alloy. These samples required no activation, most likely due to the combination of small particle size and extremely rough surfaces, which create a large surface area for hydrogen absorption. The observations that the capacities of many of the horn alloy samples is much less than the maximum reversible capacity, and these capacities did not increase with cycling, indicates that these particles have undergone irreversible oxidation resulting in a permanent loss of hydrogen storage capacity.

The exact mechanism of the oxidation is unclear, but we speculate that one contribution may be surface poisoning by water retained in the sample after nitric acid sonication. It is well known that water and oxygen impurities can deactivate titanium during hydrogen absorption-desorption cycling [11]. Specifically, TPR/TPD experiments have shown that water impurities

are consumed by titanium at temperatures above 500 K, lowering the reversible capacity by as much as 75% [11]. Clearly, from Fig. 5, a great deal of water desorbs from the lower capacity alloy samples at these high temperatures. Reaction with water at these high temperatures promotes the oxidation of titanium via the reaction:

$$Ti + 2H_2O \rightarrow TiO_2 + 2H_2, \qquad \Delta H = -428\,kJ/mol$$

Thus, this TiO_2 formation likely contributes significantly to oxidation of the tip alloy particles and the attendant loss of hydrogen capacity.

5. Conclusion

We have measured the reversible hydrogen storage capacity of a variety of Ti–6Al–4V alloy particles using temperature programmed desorption and volumetric techniques. We report the maximum hydrogen storage capacity of 3.759 ± 0.044 wt%, using small particles, and charging at standard temperature and pressure for 1 h. Experiments performed on alloy particles generated in a strongly oxidizing environment suggest that oxygen-containing species may deactivate the alloy to hydrogen storage by promoting irreversible oxidation of a fraction of the metal atoms in a sample. These results should be useful for further considerations of the Ti–6Al–4V alloy in the nuclear and hydrogen storage fields.

Acknowledgements

Funding provided by the US Department of Energy's Office of Energy Efficiency and Renewable Energy within the Hydrogen Program's Center of Excellence on Carbon-based Hydrogen Storage Materials and by the Office of Science, Basic Energy Sciences, Division of Materials Sciences and Engineering under subcontract DE-AC36-99GO10337 to NREL.

References

[1] S. Ishiyama, K. Fukaya, M. Eto, N. Miya, J. Nucl. Sci. Technol. 37 (2000) 144.
[2] Y. Hirohata, T. Oda, T. Hino, S. Sengoku, J. Nucl. Mater. 196 (2001) 290–293.
[3] X.B. Yu, Z. Wu, B.J. Xia, N.X. Xu, J. Alloys Compd. 373 (2004) 134.
[4] X.B. Yu, J.Z. Chen, Z. Wu, B.J. Xia, N.X. Xu, Int. J. Hydrogen Energy 29 (2004) 1377.
[5] A. Lopez-Suarez, J. Rickards, R. Trejo-Luna, Int. J. Hydrogen Energy 28 (2003) 1107.
[6] M.J. Heben, A.C. Dillon, K.E.H. Gilbert, P.A. Parilla, T. Gennett, J.L. Alleman, G.L. Hornyak, K.M. Jones, Hydrogen Mater. Vac. Syst. (2003) 77.
[7] E. Poirier, R. Chahine, P. Benard, D. Cossement, L. Lafi, E. Melancon, T.K. Bose, S. Desilets, Appl. Phys. A: Mater. Sci. Process. 78 (2004) 961.
[8] J. Bloch, M.H. Mintz, J. Alloys Compd. 529 (1997) 253–254.
[9] Titanium hydrides, in: W. Mueller, J.P. Blackledge, G.G. Libowitz (Eds.), Metal Hydrides, Academic Press, New York, 1968, p. 344.
[10] Y.F. Yamanaka, Y. Fujita, M. Uno, M. Katsura, J. Alloys Compd. 42 (1999) 293–295.
[11] I.N. Filimonov, V.V. Yuschenko, A.V. Smirnov, S.N. Nesterenko, I.V. Dobryakova, I.I. Ivanova, E.N. Lubnin, L. Galperin, R.H. Jensen, J. Alloys Compd. 390 (2005) 144.
[12] I.C. Corneliu, B.J. Heuser, Surf. Sci. 450 (2000) 242.
[13] A.A. Bulbich, J. Alloys Compd. 196 (1993) 29.
[14] E. Tal-Gutelmacher, D. Eliezer, Glass Phys. Chem. 31 (2005) 96.
[15] K.E.H. Gilbert, P.A. Parilla, J.B. Blackburn, A.C. Dillon, M.J. Heben, submitted for publication.
[16] IEA/DOE/SNL on-line hydride databases, http://hydpark.ca.sandia.gov.
[17] R. Wiswall, Hydrogen storage in metals, in: G. Alefeld, J. Volkl (Eds.), Topics in Applied Physics: Hydrogen in Metals II, Springer-Verlag, New York, 1978, p. 212.
[18] J. Crank, The Mathematics of Diffusion, second ed., Oxford University Press, Oxford, 1975.